Original Article

Foxa1-Deficient Mice Exhibit Impaired Insulin Secretion due to Uncoupled Oxidative Phosphorylation

Marko Z. Vatamaniuk,[1] Rana K. Gupta,[1] Kristen A. Lantz,[1] Nicolai M. Doliba,[2] Franz M. Matschinsky,[2] and Klaus H. Kaestner[1]

Foxa1 **(formerly hepatic nuclear factor 3α) belongs to the family of *Foxa* genes that are expressed in early development and takes part in the differentiation of endoderm-derived organs and the regulation of glucose homeostasis. *Foxa1*$^{-/-}$ pups are growth retarded and hypoglycemic but glucose intolerant in response to an intraperitoneal glucose challenge. However, the mechanism of glucose intolerance in this model has not been investigated. Here, we show that *Foxa1*$^{-/-}$ islets exhibit decreased glucose-stimulated insulin release in islet perifusion experiments and have significantly reduced pancreatic insulin and glucagon content. Moreover, *Foxa1*$^{-/-}$ β-cells exhibit attenuated calcium influx in response to glucose and glyburide, suggesting an insulin secretion defect either at the level or upstream of the ATP-sensitive K^+ channel. Intracellular ATP levels after incubation with 10 mmol/l glucose were about 2.5 times lower in *Foxa1*$^{-/-}$ islets compared with controls. This diminished ATP synthesis could be explained by increased expression of the mitochondrial uncoupling protein uncoupling protein 2 (UCP2) in *Foxa1*-deficient islets, resulting in partially uncoupled mitochondria. Chromatin immunoprecipitation assays indicate that UCP2 is a direct transcriptional target of *Foxa1* in vivo. Thus, we have identified a novel function for *Foxa1* in the regulation of oxidative phosphorylation in pancreatic β-cells.** ***Diabetes*** **55:2730–2736, 2006**

The *Foxa* gene family (formerly known as hepatic nuclear factor 3) plays an essential role in the development and maintenance of the endocrine pancreas (1). *Foxa2* is required for the activation of both subunits of the ATP-dependent potassium channel, as well as the expression of short-chain fatty acyl-CoA dehydrogenase (1,2). Mutations of either target have been linked to hyperinsulinemic hypoglycemia in humans (3). In addition, *Foxa2* contributes to the activation of the pancreatic duodenal homeobox 1 (IPF1 in humans), an essential regulator of both pancreatic development and β-cell function (4).

Foxa1$^{-/-}$ mice die between P2 and P12 and are hypoglycemic with no change in hepatic expression of gluconeogenic enzymes and paradoxically low levels of plasma glucagon. Pancreatic preproglucagon mRNA levels are reduced by 70% in the mutant mice (5,6). The regulation of the *glucagon* gene by *Foxa1* appears to be direct, as *Foxa1* binds to the *glucagon* gene promoter in vitro and activates its expression in cotransfection assays (5). In addition, *Foxa1*$^{-/-}$ mice display impaired glucose tolerance in response to intraperitoneal glucose injection (6). However, until now, it has not been established whether this is due to a β-cell deficiency and by what mechanism *Foxa1* might regulate insulin secretion.

Here, we evaluate consequences of *Foxa1* deletion on the function of the pancreatic β-cell. We demonstrate a profound defect in glucose-stimulated insulin secretion in perifusion assays and delineate a molecular mechanism that can, at least in part, explain this defect. We show that *Foxa1*-deficient β-cell mitochondria are partially uncoupled secondary to upregulation of uncoupling protein 2 (UCP2), an important regulator of oxidative phosphorylation and a direct transcriptional target of *Foxa1* in vivo.

RESEARCH DESIGN AND METHODS

The derivation of *Foxa1*$^{-/-}$ mice has been described previously (5). Genotyping was performed by PCR analysis using genomic DNA isolated from the tail tips of newborn mice. All studies were performed on P8 pups on an F1 hybrid of the inbred mouse strains C57BL/6 and 129SvEv after having backcrossed the *Foxa1*-null allele for 11 generations to each parental strain. The F1 hybrid is a defined genetic background and has the advantage of hybrid vigor by complementation of recessive mutations from parental strains. All mice were thus genetically uniform with the exception of the *Foxa1* locus. All procedures involving mice were conducted in accordance with approved institutional animal care and use committee protocols.

Islet isolation and culturing. Islets were isolated using collagenase (EC 3.4.24.3 Serva 17449), digested in Hanks buffer, followed by separation of islets from exocrine tissue in a Ficoll (Sigma F-9378) gradient (modified from [7]). Isolated islets were used fresh or cultured at 37°C, in 5% CO_2/95% O_2 for 3 days in RPMI-1640 medium supplemented with 10% fetal bovine serum, 2 mmol/l glutamine, 100 units/ml penicillin, 50 μg/ml streptomycin, and 10 mmol/l glucose.

Perifusion of islets and insulin release experiments. Freshly isolated islets were placed on a nylon filter in a plastic perifusion chamber (Millipore, Bedford, MA). The perifusion apparatus consisted of a water bath (37°C), a fraction collector (Waters Division of Millipore), and a computer-operated high-performance liquid chromatography system (Waters 625 LC System), which allowed programmable rates of flow and glucose concentration in the perifusate. The perifusate was a Krebs bicarbonate buffer (pH 7.4) containing 2.2 mmol/l Ca^{2+} and 0.25% BSA equilibrated with 95% O_2/5% CO_2. Islets were perifused with a ramp of 1 mmol/l glucose per min. The maximal islet secretion response was tested at the end of each experiment with 30 mmol/l KCl after washout of glucose.

From the [1]Department of Genetics and Institute for Diabetes, Obesity and Metabolism, University of Pennsylvania School of Medicine, Philadelphia, Pennsylvania; and the [2]Department of Biochemistry and Biophysics, University of Pennsylvania, Philadelphia, Pennsylvania.

Address correspondence and reprint requests to Klaus H. Kaestner, University of Pennsylvania School of Medicine, 415 Curie Blvd., Philadelphia, PA 19104-6145. E-mail: kaestner@mail.med.upenn.edu.

Received for publication 12 April 2006 and accepted in revised form 7 July 2006.

ChIP, chromatin immunoprecipitation assay; K_{ATP} channel, ATP-sensitive K^+ channel; KRBB, Krebs-Ringer bicarbonate buffer; TSS, transcriptional start site; UCP2, uncoupling protein 2.

DOI: 10.2337/db05-0470

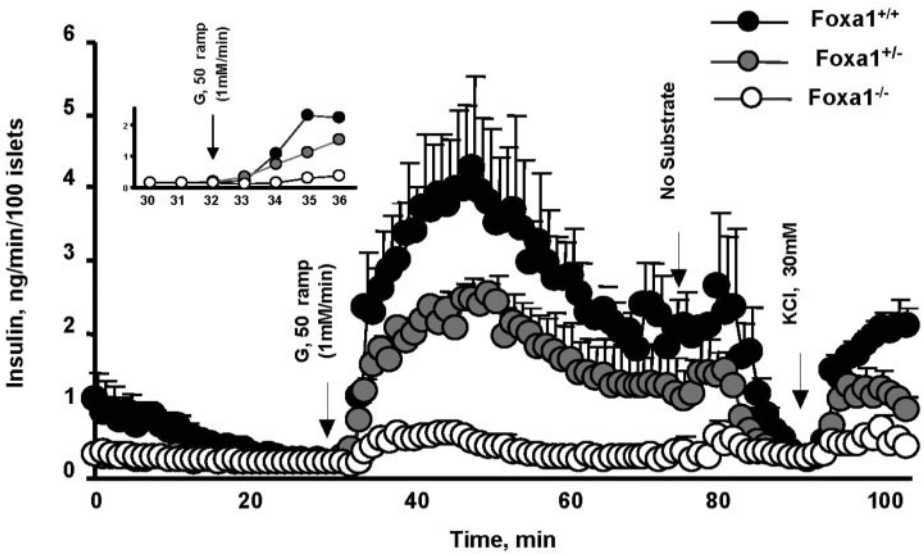

FIG. 1. Glucose-stimulated insulin release from *Foxa1*$^{+/+}$, *Foxa1*$^{+/-}$, and *Foxa1*$^{-/-}$ islets. After isolation, islets were allowed to recover and stabilize for ~30 min in KRBB containing no glucose. Then, a glucose ramp was applied progressively from 0 to 50 mmol/l, increasing glucose at 1 mmol/l per min (G). Glucose was washed out for 10 min (No Substrate) before testing islets with high concentration of potassium chloride (KCl). *Insert*: *Foxa1*$^{-/-}$ islets showed a delayed initial response to the glucose ramp compared with controls ($n = 5$).

Insulin measurements. Insulin in the effluent was measured by radioimmunoassay with charcoal separation (8). Rat insulin from Linco Research served as standard, and Miles anti-insulin antibody from ICN was the primary antibody.

Intracellular calcium measurement. Cultured P8 islets were loaded with fura-2 AM (Molecular Probes, Eugene, OR) during a 40-min pretreatment at 37°C in 2 ml of Krebs-Ringer bicarbonate buffer (KRBB) supplemented with 1 mmol/l fura-2 AM. The loaded islets were transferred to a perifusion chamber and placed on the thermo platform of an inverted Zeiss microscope. Islets were perifused with KRBB at 37°C at a flow rate of 2 ml/min, while various treatments were applied. The microscope was used with a 40× oil-immersion objective. The intracellular Ca^{2+} was determined from the ratio of the excitation of fura-2 AM at 334 and 380 nm. Emission was measured at 520 nm by an AttoFluor charge-coupled device camera and calibrated using AttoFluor Ratio Vision software.

ATP assay. Cultured islets were preincubated at 37°C for 1 h in glucose-free KRBB and then incubated in solutions with defined glucose concentration. ATP was extracted from islets and assayed as previously described (9).

Immunohistochemistry and β-cell counting. Slides were blocked with Avidin D and Biotin blocking reagents (Vector Laboratories, Burlingame, CA) for 15 min at room temperature, followed by blocking with protein-blocking reagent (Immunities, Fullerton, CA) for 20 min at room temperature. The anti-insulin antibody (Linco) was diluted 1:400 in PBS and incubated with the sections overnight at 4°C. Slides were washed in PBS and incubated with biotinylated anti-goat antibody. Horse radish peroxidase–conjugated avidin-biotin complex reagent was used following the manufacturer's protocol (Vector). Signals were developed using diaminobenzidine tetrahydtochloride as substrate. For β-cell mass determination, pancreata were laid flat during the paraffin-embedding process. The section with the largest footprint was stained for insulin by immunohistochemistry as outlined above. Quantification of β-cell area was performed as described previously (10).

RNA isolation and real-time RT-PCR. Islets isolated from three to five P8 mice of the same genotype were homogenized in 1 ml Trizol reagent (Invitrogen). Glycogen (20 μg; Roche) was added to each sample as a carrier, followed by chloroform extraction and isopropanol precipitation. After being washed with 70% ethanol, RNA pellets were resuspended in 300 μl of 10 mmol/l Tris, pH 7.5, 1 mmol/l EDTA, and 0.1% SDS. RNA was reextracted with 600 μl phenol/chloroform/isoamyl alcohol (25:24:1) and was precipitated with one-tenth volume 3 mol/l sodium acetate and 3 volumes of ethanol. RNA was quantified with the RNA 6000 nano assay program of the Agilent 2100 bioanalyzer (Agilent Technologies, Wilmington, DE), diluted with nuclease-free water, and stored at −80°C until use. Islet RNA was reversed transcribed using 1 μg Oligo (dT) primer and Superscript II Reverse Transcriptase and accompanying reagents (Invitrogen). PCR mixes were assembled using the brilliant SYBR green quantitative PCR master mix (Stratagene, La Jolla, CA). Reactions were performed using the SYBR green program on a MX 4000 quantitative PCR system (Stratagene). All reactions were performed in triplicate, and the median C_t value was used for analysis. Primer sequences are available upon request.

Evaluation of mitochondrial membrane potential. Mitochondrial membrane potential was evaluated on isolated cultured islets using ApoAlert mitochondrial membrane sensor kit (Clontech Laboratories).

Computational identification of *Foxa* binding sites in the *UCP2* promoter. The transcription regulatory element database (http://rulai.cshl.edu/cgi-bin/TRED/tred.cgi?process=analysisMatrixForm), which uses the *Foxa* position weight matrix from the JASPAR database, was used to identify *Foxa* binding sites in the proximal promoter of *UCP2*. Potential *Foxa* transcription factor binding sites were located using a cutoff score of 6.00.

Formaldehyde cross-linking and chromatin immunoprecipitation assays. Three hundred handpicked isolated islets from adult CD1 mice were suspended in 1% formaldehyde in PBS and were incubated for 10 min at room temperature while being rotated. Cross-linking was quenched by the addition of glycine to a final concentration of 0.125 mol/l, with constant shaking, for an additional 5 min. Islets were rinsed in cold PBS and lysed by rotating for 15 min at 4°C in 700 μl cell lysis buffer (10 mmol/l Tris-Cl, pH 8.0, 10 mmol/l NaCl, 3 mmol/l $MgCl_2$, and 0.5% NP-40), supplemented with protease inhibitors. Sonication was performed with a sonic dismembrator model 100 sonicator (Fisher Scientific) with a microtip probe set to a power output of 4–6 W for three cycles of 20 s each. Insoluble debris was removed by centrifugation at 13,000*g* for 10 min at 4°C, and the supernatant was collected and flash frozen in liquid nitrogen. To obtain an "input DNA" fraction, cross-linking was reversed for a 50-μl aliquot, by the addition of NaCl to a final concentration of 192 mmol/l, overnight incubation at 65°C, and purification using a Minelute PCR purification kit (Qiagen). For immunoprecipitations, 650 μl cross-linked chromatin was precleared by incubation for 1 h at 4°C with 125 μl protein G–agarose (Upstate Biotechnology, Lake Placid, NY) in a total volume of 1 ml chromatin immunoprecipitation assay (ChIP) dilution buffer (20 mmol/l Tris-HCl, pH 8.1, 1% Triton X-100, 2 mmol/l EDTA, and 150 mmol/l NaCl). After this preclearing, the supernatant was evenly divided and incubated overnight with *Foxa1*-specific antiserum (kind gift of G. Schütz, Heidelberg, Germany) or control IgG. Immunoprecipitation was performed as described (11). The precipitated and un–cross-linked DNA was purified on a Minelute purification column and eluted in 30 μl 10 mmol/l Tris, pH 8.5. Primer sequences for PCR are available upon request.

Electrophoretic mobility shift assays. Oligonucleotides were synthesized corresponding to the *Foxa* binding sites in the *UCP2* promoter. Radiolabeled probes were generated by incubation of 250 ng annealed oligonucleotides with 20 μCi ^{32}P-dCTP in the presence of Klenow DNA polymerase (Roche Applied Science, Indianapolis, IN) for 15 min at 37°C. Radiolabeled probes were subsequently separated from free nucleotide using G-50 column purification (Amersham). Liver nuclear extract was then incubated at room temperature for 15 min with a 100,000-dpm radiolabeled probe and 1 μg poly(dI-dC) in 10 mmol/l Tris-HCl, pH 7.5, 50 mmol/l NaCl, 1 mmol/l dithiothreitol, 1 mmol/l EDTA, and 5% glycerol. Some binding reactions were subsequently incubated

with anti-*Foxa1/2* antibody (Santa Cruz sc-6553) for 30 min at room temperature. Samples were resolved on 5% polyacrylamide gels in 0.5% Tris-borate-EDTA at 300 V for 2 h. The dried gel was exposed to a phosphorimager cassette (Amersham) and analyzed with Storm840 software (Amersham). Oligonucleotide sequences for the *Foxa* sites in the *UCP2* promoter: −1,760 bp forward, 5′-GGGGAAAAAGATTTATTTATTTTATGTA-3′; −1,760 bp reverse, 5′-GGGGTACATAAAATAAATAAATCTTTTT-3′; −1,639 bp forward, 5′-GGGGGAGTCCAAAAATTTATTTATAACT-3′; −1,639 bp reverse, 5′-GGGGAGT TATAAATAAATTTTTGGACTC-3′.

RESULTS

Mice deficient for the winged helix transcription factor *Foxa1* are hypoglycemic (5) but have reduced plasma insulin levels after intraperitoneal glucose challenge (6). However, the molecular mechanism of this apparent insulin secretory effect has not yet been investigated. We used the islet perifusion technique in order to evaluate insulin release from isolated *Foxa1*$^{-/-}$, *Foxa1*$^{+/-}$, and wild-type islets in response to glucose challenge. *Foxa1*-deficient islets exhibited dramatically reduced glucose-stimulated insulin release (Fig. 1). The maximum rate of insulin release in response to high glucose was ~10 times lower compared with the wild-type islets. In addition, mutant islets showed a right shift in their response to glucose (Fig. 1), requiring higher glucose levels to initiate the first-phase response. At the end of every experiment, the functional integrity of the islets was confirmed by the secretory response to KCl depolarization. Interestingly, the KCl response was apparent, but consistently reduced in *Foxa1*$^{-/-}$ islets compared with the controls.

The reduced insulin secretory response of *Foxa1*$^{-/-}$-deficient β-cells, even when depolarized completely by KCl, raised the question of whether insulin content is dependent on *Foxa1*. Indeed, we found that total pancreatic insulin content normalized to pancreatic mass was approximately three times lower (533 ± 96 vs. 154 ± 14 ng/mg pancreas), and total glucagon content was reduced ~2.5-fold (48 ± 9 vs. 20 ± 1 pg/mg pancreas) in *Foxa1*$^{-/-}$ compared with wild-type pancreata (Fig. 2*A* and *B*). This reduction in total insulin content could be due to a reduction in β-cell mass or a decrease of the amount of insulin per cell. To address this issue, we determined pancreatic β-cell area by point-counting morphometry. β-Cell area was not significantly changed in *Foxa1*$^{-/-}$ mice (Fig. 2*C*), suggesting that the defect lies in the amount of insulin per β-cell. Consistent with this notion, insulin mRNA levels in isolated islets were reduced by ~50% in *Foxa1*$^{-/-}$-deficient mice (Fig. 2*D*). Thus, while the initial specification of pancreatic β-cells does not require *Foxa1*, terminal differentiation into fully mature β-cells is dependent on *Foxa1* expression.

Given the striking defect in insulin secretion documented above, it appeared unlikely that the modestly reduced insulin content fully explains the defect in glucose-stimulated insulin release. Thus, we proceeded to identify additional defects, which may contribute to the reduction in insulin release. First, we measured changes in intracellular calcium levels in response to various secretagogues in mutant and in control islets using fluorescent calcium chelators and dual-wavelength fluorescent microscopy. Glucose, as well as the ATP-sensitive K^+ channel (K_{ATP} channel) blocker glyburide, evoked the expected calcium entry into control islets (Fig. 3*A*), while the same stimuli were significantly less potent in the absence of *Foxa1* (Fig. 3*B*). These results suggested a defect in metabolism upstream of calcium inflow into the β-cell in *Foxa1*$^{-/-}$ mice. Calcium entry into the cell under normal

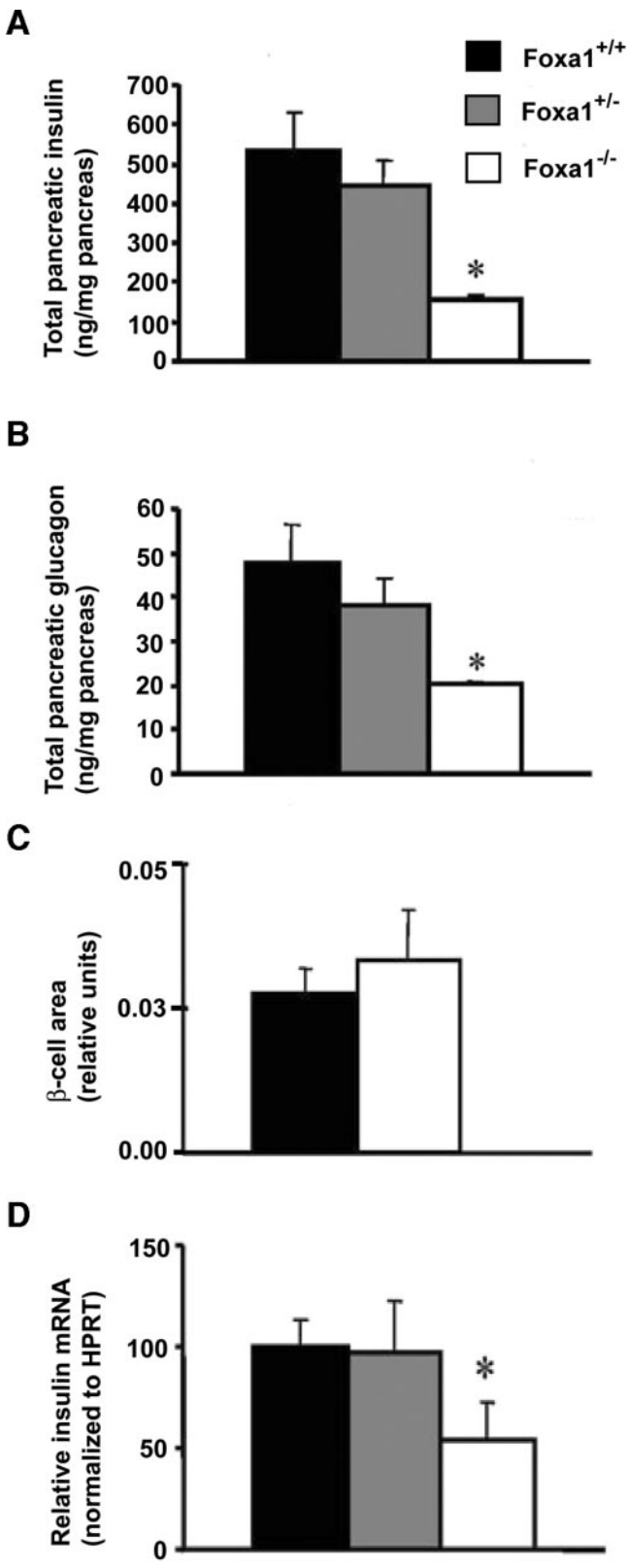

FIG. 2. Insulin and glucagon content in total pancreata of *Foxa1*$^{+/+}$, *Foxa1*$^{+/-}$, and *Foxa1*$^{-/-}$ mice. Insulin and glucagon concentrations were estimated in total pancreata of controls and mutants after acid-alcohol extraction. Total insulin (*A*) and glucagon content (*B*) were significantly reduced in *Foxa1*$^{-/-}$ pancreas compared with controls ($n = 5$). *C*: The ratio of β-cell area to total pancreatic area is not changed in *Foxa1*$^{-/-}$-deficient mice compared with littermate controls ($n = 5$). *D*: Insulin mRNA levels. *Foxa1*-deficient mice have a twofold lower level of islets of insulin mRNA compared with controls. mRNA levels were normalized to mRNA levels of hypoxanthine phosphoribosyl transferase (HPRT). *$P < 0.05$ by Student's *t* test.

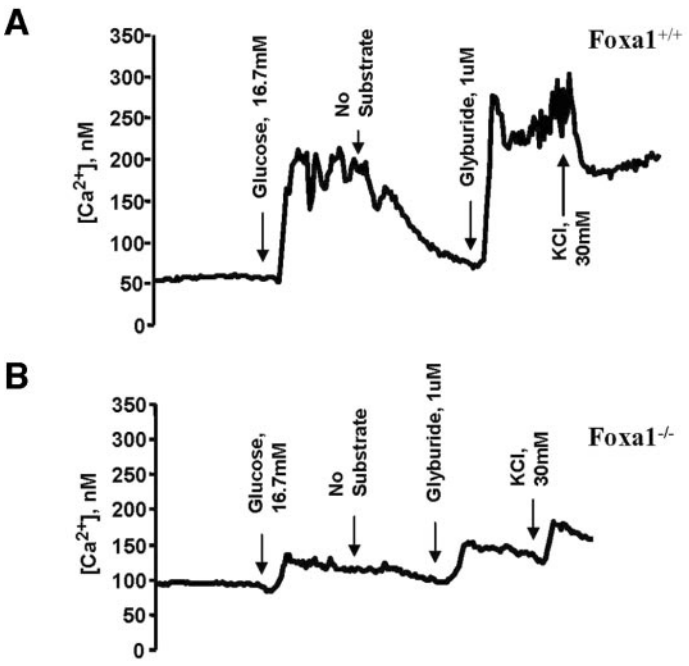

FIG. 3. Intracellular Ca^{2+} in islets of *Foxa1*$^{+/+}$ and *Foxa1*$^{-/-}$ mice. Isolated islets were cultured with 10 mmol/l glucose for 3 days on cover slips. Intracellular Ca^{2+} was measured by fura-2 fluorescence in response to high glucose and the K_{ATP} channel blocker glyburide. *A*: Typical response to glucose and glyburide in *Foxa1*$^{+/+}$ islets. *B*: Diminished intracellular Ca^{2+} response of *Foxa1*$^{-/-}$ islet to the same stimuli. The highest response out of all *Foxa1*$^{-/-}$ tested islets is represented and is one of five experiments performed with similar results.

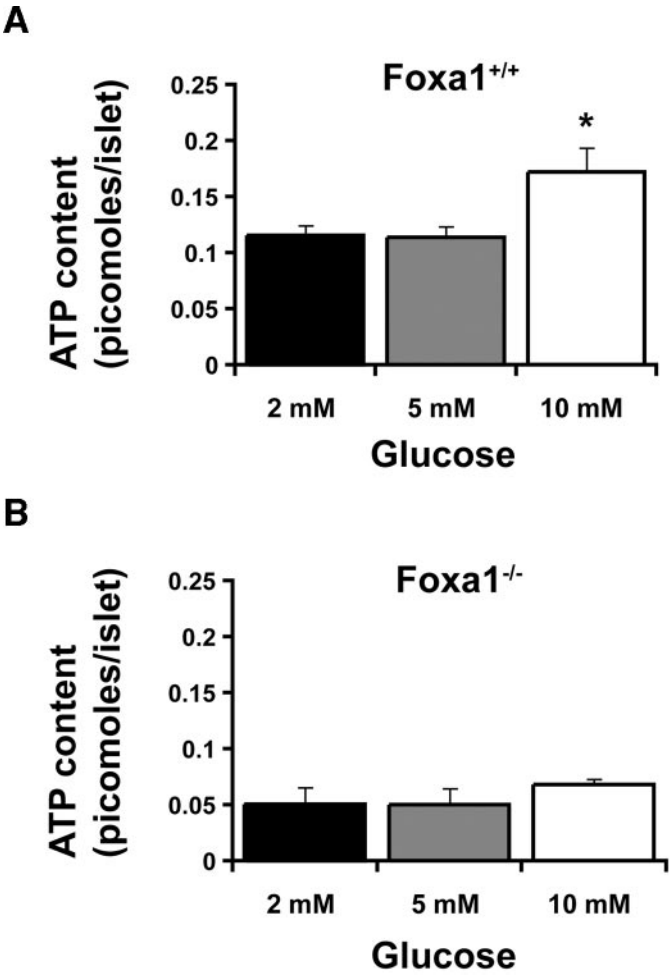

FIG. 4. ATP levels in islets isolated from *Foxa1*$^{+/+}$ and *Foxa1*$^{-/-}$ mice. Isolated islets were cultured with 10 mmol/l glucose for 3 days. Islets were cultured for 1 h without glucose, followed by 1 h incubation with 2, 5, or 10 mmol/l glucose. *A*: ATP levels were elevated in control islets after incubation with 10 mmol/l glucose compared with 2 or 5 mmol/l. *B*: *Foxa1*$^{-/-}$ islet ATP levels did not change significantly under the same conditions. The ATP levels per islet shown here are about 10-fold less than those obtained for adult islets due to the fact that the islets from P8 mice have, on average, only one-tenth the volume of adult islets.

physiological conditions depends on energy metabolism and the subsequent closure of ATP-dependent potassium channels. Therefore, we assessed ATP levels in islets of control and *Foxa1*$^{-/-}$ mice exposed to various concentrations of glucose. As expected, the ATP content in control islets was increased significantly in response to 10 mmol/l glucose (Fig. 4*A*). In contrast, ATP concentrations of *Foxa1*$^{-/-}$ islets were not increased significantly after incubation with 10 mmol/l glucose (Fig. 4*B*). In addition, ATP concentrations in *Foxa1*$^{-/-}$-deficient islets were lower than those of control mice at 2 and 5 mmol/l of glucose. The ATP levels per islet in our P8 islets are about 10-fold lower than those published for adult islets (12,13) because the islets in newborn mice are much smaller than those of adult mice.

The deficit in glucose-stimulated ATP production in the cell must reflect defects in glucose catabolism or oxidative phosphorylation. We investigated the mRNA expression of multiple enzymes involved in glucose metabolism, including GLUT2, glucokinase, phosphofruktokinase-2, glyceraldehyde-3-phosphate dehydrogenase, and pyruvate kinase in isolated control and *Foxa1* mutant islets by real-time RT-PCR. While most mRNA levels were unchanged, some showed a trend toward increased expression in *Foxa1*-deficient islets, perhaps indicating a compensatory response to attenuated ATP production (Fig. 5*A*). Thus, a defect in glucose catabolism is not a likely cause for the defect in glucose-stimulated insulin secretion in our model. However, we found a statistically significant, nearly twofold increase in the expression of UCP2, a mitochondrial uncoupling protein, in *Foxa1*$^{-/-}$ islets (Fig. 5*A*). These findings suggest the following model of perturbed glucose metabolism and insulin secretion for *Foxa1*-deficient β-cells: absence of *Foxa1* leads to increased expression of the uncoupling protein UCP2, which results in insufficient ATP production from glucose, as mitochondrial oxidative phosphorylation is partially uncoupled. Changes in glucose concentrations are then no longer translated efficiently into increased ATP levels, activation of the ATP-dependent potassium channel, and insulin release.

To prove our notion that oxidative phosphorylation in *Foxa1*$^{-/-}$ islets is uncoupled, we assessed mitochondrial membrane potential in control and mutant islets, using membrane potential–sensitive fluorescent dies. Dye aggregates are formed in healthy mitochondria with a large membrane potential and fluoresce red, while at low membrane potential the fluorescent dye monomers stay in cytosol and glow green. The red color emitted from *Foxa1*$^{+/+}$ islets reflects high mitochondrial membrane potential and is indicative of coupled respiration and oxidative phosphorylation (Fig. 5*B*). In contrast, mitochondria of *Foxa1*$^{-/-}$ islets were uncoupled as evidenced by the green fluorescence (Fig. 5*B*). Thus, the twofold increase in UCP2 expression observed in *Foxa1*$^{-/-}$ islets

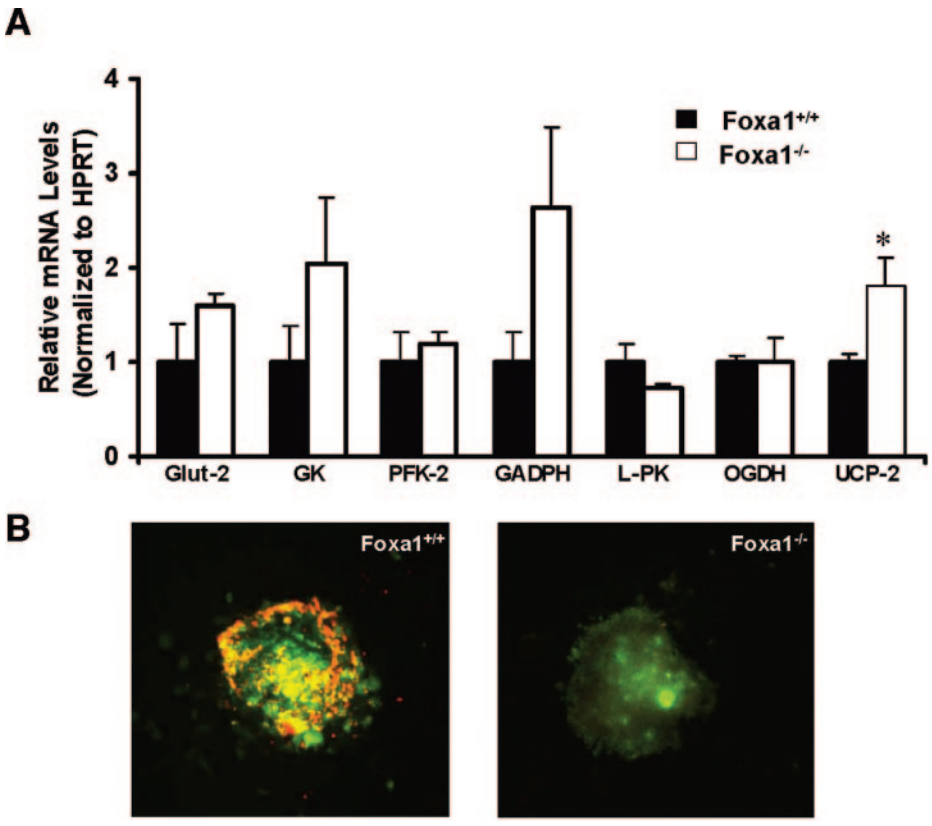

FIG. 5. Gene expression analysis. *A*: mRNA levels of genes involved in glucose metabolism were determined by real-time PCR in RNA samples from isolated islets. mRNA levels were normalized to mRNA levels of hypoxanthine phosphoribosyl transferase (HPRT). *$P < 0.05$ ($n = 5$ for each experiment). GADPH, glyceraldehyde 3-phosphate dehydrogenase; GK, glucokinase; L-PK, liver pyruvate kinase; OGDH, oxoglutarate dehydrogenase; PFK-2, phosphofruktokinase 2; UCP2, uncoupling protein 2. *B*: Mitochondrial membrane potential in *Foxa1*$^{+/+}$ and *Foxa1*$^{-/-}$ isolated islets. MitoSensor aggregates in the mitochondria with high membrane potential of wild-type *Foxa1*$^{+/+}$ islets produce red fluorescence. The absence of red fluorescence in *Foxa1*$^{-/-}$ islets is indicative of reduced mitochondrial membrane potential.

correlates with decreased membrane potential indicative of uncoupled oxidative phosphorylation.

Next, we investigated whether *UCP2* is a direct transcriptional target of *Foxa1*. First, we examined the proximal promoter of *UCP2* for potential *Foxa* binding sites, as previous studies have indicated that this region contains important regulatory elements for *UCP2* expression (14). Computational analysis identified two high-scoring *Foxa* binding sites located ~1.7 kb upstream of the transcriptional start site (TSS) (Fig. 6*A*). To determine if *Foxa1* occupies the *UCP2* promoter in islets, we performed ChIP using *Foxa1*-specific antiserum. ChIP from isolated mouse islets followed by PCR using primers (ChIP primer 1) selectively amplifying this region revealed that *Foxa1* binds 1.7 kb upstream of the TSS. Primers (ChIP primer 2) amplying a region located 700 bp upstream of the TSS, which did not contain high-scoring *Foxa* sites, were used as a negative control (Fig. 6*B*).

Under the experimental conditions described above, sonication of cross-linked chromatin produces an average DNA length of ~500 bp (data not shown). Thus, PCR of the immunoprecipitated DNA alone cannot determine which of the two putative *Foxa* binding sites located 1.7 kb upstream of the TSS represents true *Foxa* binding sites. Thus, we performed electrophoretic mobility shift assays. Incubation of liver nuclear extract with a radiolabeled oligonucleotide containing a known *Foxa* binding sequence resulted in a strong shift of the radioactive band. Addition of *Foxa* antibody generated a supershifted band that was not observed with the addition of preimmune serum, indicating that the bound protein is indeed a *Foxa* protein. However, the intensity of the shifted band was strongly diminished with the addition of an unlabeled competitor oligonucleotide containing the *Foxa* recognition sequence beginning at −1,760 bp but only weakly with the addition of an unlabeled probe containing the putative binding site at −1,639 bp (Fig. 6*C*). Thus, *Foxa1* binds to the *UCP2* promoter at a preferred site located between −1,760 and −1,749 bp relative to the transcriptional start site of the gene.

DISCUSSION

An important role for *Foxa1* in insulin secretion or action had been suggested by an abnormal response to intraperitoneal glucose challenge in *Foxa1*-deficient mice (6); however, the mechanistic nature of this defect has not been investigated previously. Here, we demonstrate that *Foxa1*-deficient islets have severely impaired glucose-stimulated insulin secretion. In addition to a dramatically decreased maximal secretion response, the onset of insulin secretion is also delayed. While β-cell area is unaffected by the loss of *Foxa1*, insulin content and insulin gene expression is reduced in islets of *Foxa1*$^{-/-}$ mice. Thus, terminal differentiation of fully mature β-cells is dependent on *Foxa1*. At present, it remains unclear how insulin mRNA levels are altered in the absence of *Foxa1*. To investigate whether *Foxa1* might be a transcriptional activator of the mouse insulin genes, we performed cotransfection assays with reporter constructs driven by both the mouse *Insulin-1*

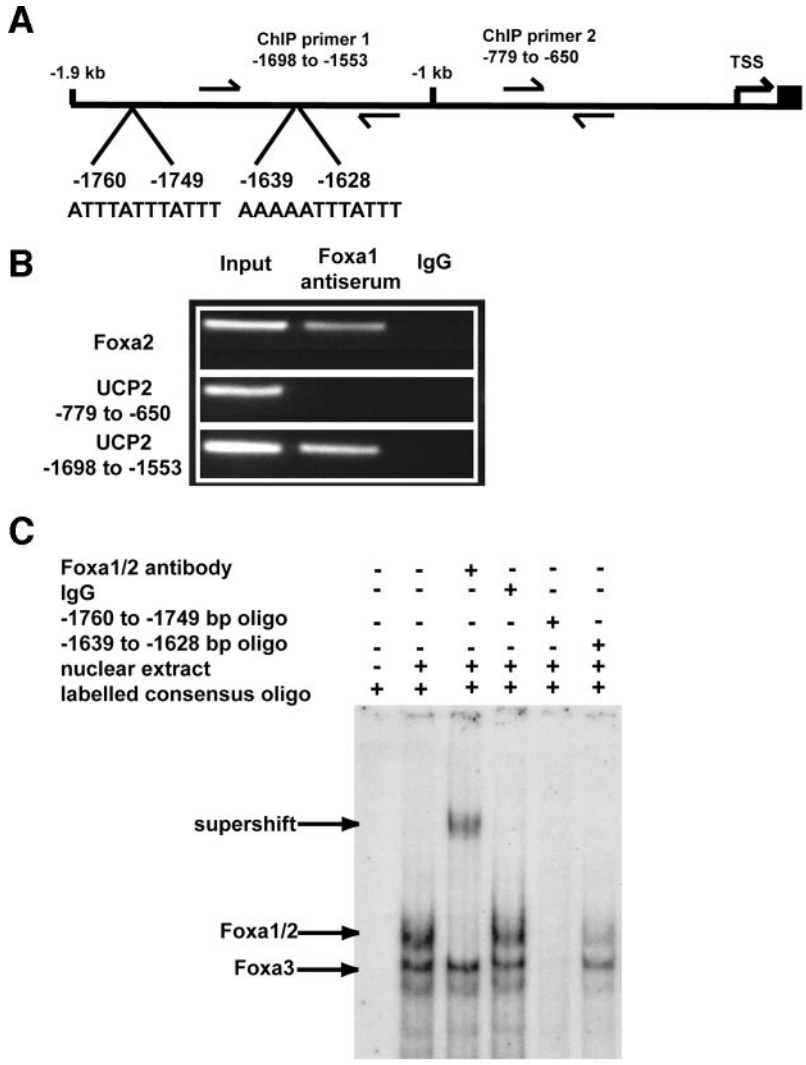

FIG. 6. *UCP2* is a direct transcriptional target of *Foxa1* in islets in vivo. *A*: Genomic organization of the mouse *UCP2* locus with putative *Foxa1* binding sites shown. Position of binding site is relative to TSS. Arrows indicate location of primer pairs used for chromatin immunoprecipitation assays. *B*: ChIP from isolated adult islets using *Foxa1*-specific antiserum reveals that *Foxa1* occupies the region 1.7-kb upstream of the TTS but does not occupy the region 800-bp upstream of the TSS. Primers amplifying known *Foxa1* binding site at *Foxa2* locus serves as a postive control for the *Foxa1* ChIP assay. *C*: Electrophoretic mobility shift assays. Incubation of liver nuclear extract with a radiolabeled oligonucleotide containing a known *Foxa* binding site resulted in a strong shift of the radioactive band. Addition of *Foxa* antibody generated a supershifted band that was not observed with the addition of preimmune serum, confirming the identity of the bound protein. Intensity of the shifted band was diminished with the addition of an unlabeled competitor oligonucleotide containing the *Foxa* binding site located 1,760-bp upstream of the TSS of *UCP2* but not diminished with unlabeled competitor oligonucleotide containing the *Foxa* binding site located 1,639-bp upstream of the TSS.

and *Insulin-2* genes. However, we were unable to find significant activation of these reporters by *Foxa1* cotransfection (data not shown). In addition, computational analysis of the insulin gene promoters failed to identify consensus *Foxa* binding sites. Therefore, it is likely that changes in insulin gene expression in *Foxa1*$^{-/-}$-deficient islets are a secondary consequence of the loss of *Foxa1*.

The first phase of insulin release depends on the activity of the K_{ATP} channel, which in turn depends on the efficient utilization of glucose and the production of ATP. We found a major defect in glucose-dependent ATP production in *Foxa1*-deficient islets. Initially, we investigated genes involved in glycolysis as potential *Foxa1* targets. However, we found that expression of these genes is unchanged or even slightly increased in the absence of *Foxa1*, which would be expected to result in unchanged or elevated ATP production from glycolysis. Thus, a defect in glycolysis does not explain the failure to secrete insulin in response to glucose observed in *Foxa1*$^{-/-}$ mice.

The insulin secretion defect in *Foxa1*$^{-/-}$ mice can be explained by the upregulation of UCP2. UCP2 belongs to a small family of natural uncouplers of respiration and oxidative phosphorylation. Originally thought to function mainly in thermogenesis by brown adipose tissue, *UCP2* gene expression in pancreatic β-cells is an important determinant of the sensitivity of insulin secretion to changes in glucose levels. Pancreatic islets isolated from UCP2-deficient animals secrete more insulin and demonstrate higher levels of ATP (13), while UCP2 overexpression in cultured rat islets leads to severe blunting in glucose-stimulated insulin secretion (12). Importantly, it has been demonstrated in several models that even small changes in UCP2 mRNA expression result in changes in glucose homeostasis. For instance, the 50% reduction in UCP2 mRNA levels in *UCP2*$^{+/-}$ mice resulted in a twofold increase in plasma insulin levels (13), thus relatively small changes in UCP2 expression, like the one we demonstrated above, are of functional significance.

Through chromatin immunoprecipitation and electrophoretic mobility shift assays, we demonstrate that *UCP2* is a direct target of *Foxa1*. *Foxa* proteins are primarily considered activators of transcription; therefore, it is unlikely that *Foxa1* functions to directly repress *UCP2* transcription. However, *Foxa* proteins, by altering chromatin structure, are known to facilitate binding of other transcription factors to DNA (15,16). We have previously shown that *Foxa2* promotes binding of cAMP-responsive element–binding protein and glucocorticoid receptor to chromatin targets in the fasting liver (17). Other studies indicate that *Foxa1* is required for binding of the estrogen receptor to cognate response elements (18,19). Recent studies indicate that Sirt1 is a potent transcriptional repressor of *UCP2* gene expression in islets (20). Sirt1 expression levels are not reduced in islets of *Foxa1*$^{-/-}$ mice (data not shown); however, interestingly, Sirt1 occupies the *UCP2* promoter in close proximity to the *Foxa1* binding site shown above (20). Thus, it is tempting to speculate that the binding of a transcriptional repressor, such as Sirt1, to the *UCP2* promoter is *Foxa1* dependent. Future experiments will examine the biochemical mechanisms by which *Foxa1* mediates the repression of *UCP2* gene expression.

In summary, we have established a novel role for *Foxa1* in the pancreatic β-cell and have shown that *Foxa1* is required for efficient coupling of oxidative phosphorylation by limiting *UCP2* gene expression.

ACKNOWLEDGMENTS

This work was supported by National Institute of Diabetes and Digestive Kidney Diseases Grant R01-DK55342 (to K.H.K.).

We are grateful to the Penn Morphology Core (P30DK50306) and Dr. Gary P. Swain for the help in developing a method for visualization of mitochondrial membrane potential in isolated pancreatic islets, the Penn RIA Core (P30DK19525) and Dr. Heather Collins for performing radioimmune assays, James Fulmer for maintaining mice the colony, and Dr. Nir Rubins for assistance with electrophoretic mobility shift assays. We also thank Drs. Joshua R. Friedman and Olga T. Hardy for critically reading the manuscript.

REFERENCES

1. Lantz KA, Kaestner KH: Winged-helix transcription factors and pancreatic development. *Clin Sci (Lond)* 108:195–204, 2005
2. Sund NJ, Vatamaniuk MZ, Casey M, Ang SL, Magnuson MA, Stoffers DA, Matschinsky FM, Kaestner KH: Tissue-specific deletion of Foxa2 in pancreatic beta cells results in hyperinsulinemic hypoglycemia. *Genes Dev* 15:1706–1715, 2001
3. Molven A, Matre GE, Duran M, Wanders RJ, Rishaug U, Njolstad PR, Jellum E, Sovik O: Familial hyperinsulinemic hypoglycemia caused by a defect in the SCHAD enzyme of mitochondrial fatty acid oxidation. *Diabetes* 53:221–227, 2004
4. Lee CS, Sund NJ, Vatamaniuk MZ, Matschinsky FM, Stoffers DA, Kaestner KH: *Foxa2* controls *Pdx1* gene expression in pancreatic β-cells in vivo. *Diabetes* 51:2546–2551, 2002
5. Kaestner KH, Katz J, Liu Y, Drucker DJ, Schutz G: Inactivation of the winged helix transcription factor HNF3alpha affects glucose homeostasis and islet glucagon gene expression in vivo. *Genes Dev* 13:495–504, 1999
6. Shih DQ, Navas MA, Kuwajima S, Duncan SA, Stoffel M: Impaired glucose homeostasis and neonatal mortality in hepatocyte nuclear factor 3alpha-deficient mice. *Proc Natl Acad Sci U S A* 96:10152–10157, 1999
7. Scharp DW, Kemp CB, Knight MJ, Ballinger WF, Lacy PE: The use of ficoll in the preparation of viable islets of langerhans from the rat pancreas. *Transplantation* 16:686–689, 1973
8. Herbert VLK, Gottlieb CW, Bleicher SJ: Coated charcoal immunoassay of insulin. *J Clin Endocrinol Metab* 25:1375–1384, 1965
9. Li C, Najafi H, Daikhin Y, Nissim IB, Collins HW, Yudkoff M, Matschinsky FM, Stanley CA: Regulation of leucine-stimulated insulin secretion and glutamine metabolism in isolated rat islets. *J Biol Chem* 278:2853–2858, 2003
10. Bonner-Weir S: Regulation of pancreatic beta-cell mass in vivo. *Recent Prog Horm Res* 49:91–104, 1994
11. Rubins NE, Friedman JR, Le PP, Zhang L, Brestelli J, Kaestner KH: Transcriptional networks in the liver: hepatocyte nuclear factor 6 function is largely independent of Foxa2. *Mol Cell Biol* 25:7069–7077, 2005
12. Chan CB, De Leo D, Joseph JW, McQuaid TS, Ha XF, Xu F, Tsushima RG, Pennefather PS, Salapatek AMF, Wheeler MB: Increased uncoupling protein-2 levels in β-cells are associated with impaired glucose-stimulated insulin secretion: mechanism of action. *Diabetes* 50:1302–1310, 2001
13. Zhang C-Y, Baffy G, Perret P, Krauss S, Peroni O, Grujic D, Hagen T, Vidal-Puig AJ, Boss O, Kim Y-B: Uncoupling protein-2 negatively regulates insulin secretion and is a major link between obesity, beta-cell dysfunction, and type 2 diabetes. *Cell* 105:745–755, 2001
14. Medvedev AV, Snedden SK, Raimbault S, Ricquier D, Collins S: Transcriptional regulation of the mouse uncoupling protein-2 gene: double E-box motif is required for peroxisome proliferator-activated receptor-gamma-dependent activation. *J Biol Chem* 276:10817–10823, 2001
15. Cirillo LA, Lin FR, Cuesta I, Friedman D, Jarnik M, Zaret KS: Opening of compacted chromatin by early developmental transcription factors HNF3 (FoxA) and GATA-4. *Mol Cell* 9:279–289, 2002
16. Gualdi R, Bossard P, Zheng M, Hamada Y, Coleman JR, Zaret KS: Hepatic specification of the gut endoderm in vitro: cell signaling and transcriptional control. *Genes Dev* 10:1670–1682, 1996
17. Zhang L, Rubins NE, Ahima RS, Greenbaum LE, Kaestner KH: Foxa2 integrates the transcriptional response of the hepatocyte to fasting. *Cell Metab* 2:141–148, 2005
18. Carroll JS, Liu XS, Brodsky AS, Li W, Meyer CA, Szary AJ, Eeckhoute J, Shao W, Hestermann EV, Geistlinger TR, Fox EA, Silver PA, Brown M: Chromosome-wide mapping of estrogen receptor binding reveals long-range regulation requiring the forkhead protein FoxA1. *Cell* 122:33–43, 2005
19. Laganiere J, Deblois G, Lefebvre C, Bataille AR, Robert F, Giguere V: From the cover: location analysis of estrogen receptor alpha target promoters reveals that FOXA1 defines a domain of the estrogen response. *Proc Natl Acad Sci U S A* 102:11651–11656, 2005
20. Bordone L, Motta MC, Picard F, Robinson A, Jhala US, Apfeld J, McDonagh T, Lemieux M, McBurney M, Szilvasi A, Easlon EJ, Lin SJ, Guarente L: Sirt1 regulates insulin secretion by repressing UCP2 in pancreatic beta cells. *PLoS Biol* 4:e31, 2006